



Simple optical measurement of the magnetic moment of magnetically labeled objects



Alexandra Heidsieck^{a,*}, Sarah Rudigkeit^b, Christine Rümenapp^a, Bernhard Gleich^a

^a Zentralinstitut für Medizintechnik, Technische Universität München, Germany

^b Physics Department, Technische Universität München, Germany

ARTICLE INFO

Keywords:

Magnetic moment
Magnetization
Magnetic nanoparticles
Velocity measurement
Magnetophoretic mobility
Characterization

ABSTRACT

The magnetic moment of magnetically labeled cells, microbubbles or microspheres is an important optimization parameter for many targeting, delivery or separation applications. The quantification of this property is often difficult, since it depends not only on the type of incorporated nanoparticle, but also on the intake capabilities, surface properties and internal distribution.

We describe a method to determine the magnetic moment of those carriers using a microscopic set-up and an image processing algorithm. In contrast to other works, we measure the diversion of superparamagnetic nanoparticles in a static fluid. The set-up is optimized to achieve a homogeneous movement of the magnetic carriers inside the magnetic field. The evaluation is automated with a customized algorithm, utilizing a set of basic algorithms, including blob recognition, feature-based shape recognition and a graph algorithm. We present example measurements for the characteristic properties of different types of carriers in combination with different types of nanoparticles. Those properties include velocity in the magnetic field as well as the magnetic moment. The investigated carriers are adherent and suspension cells, while the used nanoparticles have different sizes and coatings to obtain varying behavior of the carriers.

1. Introduction

Magnetically labeled cells, microbubbles or microspheres have become important tools for targeting, delivery or separation applications. Magnetic nanoparticles experience a force in an inhomogeneous magnetic field and are drawn towards the magnetic field source. Thereby, they can be diverted by an external magnetic field gradient. Magnetically labeled cells, microbubbles or microspheres incorporate up to several hundred magnetic nanoparticles and can thereby be manipulated more effectively by external magnetic fields.

However, the magnetic properties of those objects are often not quantified. In order to optimize the application and judge the efficiency, the magnetic moment of the objects must be known. This property can only be measured indirectly by observing the objects in a well-defined and known magnetic field. Most of the known methods to measure the magnetic moment of nanoparticles and magnetically labeled objects focus on the magnetization of the particles or the magnetic moment of a bulk of particles. Among the most commonly used methods are magnetization [1], force [2,3] and direct [4–6] or indirect [7,8] optical velocity measurements.

Since we are interested in the magnetic moment of the individual

objects, we utilized optical velocity measurements. Complexes of nanoparticles, microspheres or cells, which are large enough to be seen under a microscope, can be tracked optically in a magnetic field. Häfeli et al. [4] as well as Zborowski and Chalmers et al. [5,6] used this method to track magnetic microspheres and magnetically labeled cells in a magnetic force field. This is also known as “Cell Tracking Velocimetry” or “Particle Tracking Velocimetry”. The measured quantity is often called “magnetophoretic mobility” and refers to the velocity of the objects normalized by the magnetic field. The magnetic set-ups vary from complex electromagnets to single large permanent magnets. Often, the cells are carried along by a laminar flow and diverted by a magnetic force perpendicular to their streamline. Based on the deviation from their original path, the magnetophoretic mobility and thereby the magnetic moment of the particles can be determined. While most available cell tracking velocimetry set-up can accomplish that, they are large and expensive. We aimed to design a simple set-up of a manageable size which can be used in any laboratory where a microscope with a digital camera is available.

Additionally, we aimed for a homogeneous force on the objects for the measurement of the magnetic moment to avoid acceleration. In the following, we present a method which is able to measure the magnetic

* Corresponding author.

E-mail address: ahheidsieck@tum.de (A. Heidsieck).

moment of magnetic nanoparticle complexes, microbubbles and cells, based on the observation of their movement under well-defined conditions. Based on a Halbach cylinder, we developed a magnetic set-up in which the carriers move with a nearly constant velocity. Particle complexes, microbubbles or cells are added to a fluid in a high, but homogeneous magnetic flux density gradient field. Thereby, a homogeneous movement of the objects is assured. We observe the movement via optical microscopy and are able to draw conclusions about the magnetic moment of the object.

2. Theory

The magnetization \vec{M} describes the strength of the magnetic dipole moment of the nanoparticle at a defined magnetic field strength and is defined as magnetic moment $\vec{\mu}$ per volume of the core material. Thereby, magnetic moment and magnetization are dependent on each other. Furthermore, the magnetization, as well as the magnetic moment depend on the strength of the external magnetic flux density field.

The magnetic force acting on a magnetically labeled object with the magnetic dipole moment $\vec{\mu}$ within an external inhomogeneous, static magnetic flux density field \vec{B} is described by

$$\vec{F}_{\text{mag}} = (\vec{\mu} \cdot \nabla) \vec{B} \quad (1)$$

and can – for an external, static magnetic field – be simplified to

$$\vec{F}_{\text{mag}} = \mu(B) \cdot \nabla B \quad (2)$$

where the absolute value of the magnetic dipole moment $\mu = |\vec{\mu}|$ of a superparamagnetic nanoparticle depends on the absolute value of the local magnetic flux density $B = |\vec{B}|$ and can be described by

$$\mu(B) = \mu_{\text{sat}} L(B) \quad (3)$$

where L is the Langevin function [9]

$$L(B) = \coth\left(\frac{\mu_{\text{sat}} B}{k_B T}\right) - \frac{k_B T}{\mu_{\text{sat}} B} \quad (4)$$

and μ_{sat} is the saturation magnetization of the particles.

While the magnetization is usually constant for the same particle type at a certain flux density, the magnetic moment varies with the particle size. For larger objects which incorporate a larger amount of nanoparticles, we assume that the magnetic moment is proportional to the hydrodynamic surface area or volume of the object which are referred to as volume magnetization M_V and surface magnetization M_A .

The movement of the object with a velocity v causes friction between object and fluid which is described by the Stokes' drag force

$$\vec{F}_{\text{hydro}} = 3\pi\eta d_h \vec{v}, \quad (5)$$

where η denotes the viscosity of the fluid and d_h is the hydrodynamic diameter of the corresponding object.

3. Materials and methods

3.1. Cell culture and media

MDA cells were maintained in complete culture medium composed of Dulbecco's Modified Eagle medium high glucose (DMEM, Biochrom) supplemented with 1 mM sodium pyruvate (Na-pyruvate (100 mM), Biochrom), 5% foetal bovine serum (FBS, Hyclone, perbio) and 0.1% Pen/Strep (Biochrom). Cells were passaged every 7 days at 2500 cells/cm² using Trypsin/EDTA-solution (0.05% /0.02%) in PBS w/o Ca²⁺/Mg²⁺ (Biochrom) and 1 x PBS. Cell preparations were maintained at standard cell culture conditions 37 °C, 5% CO₂ and 95% humidity incubator (HERAEUS, Hanau, Germany).

3.2. Magnetic nanoparticles

The cells were loaded with three different types of magnetic nanoparticles:

- SO-Mag5 is a multi-core MNP made of maghemite cores closed up in a silica shell with a diameter of approximately 40 ± 14 nm. [10].
- MNP are bare magnetic nanoparticles made of maghemite with a distribution of the diameter of 5 ± 2 nm [11].
- MNP-APTES are MNP coated with (3-Aminopropyl)-triethoxysilane (APTES) (abcr GmbH) after the protocol of Ma et al. leaving free amino groups on their surface [12]. 10 ml of the bare particles were diluted in 10 ml of H₂O_{dd} and degased in an ultrasound bath for 15 min. Afterwards EtOH (absolute, Applichem GmbH) was added to the particles in a concentration of 0.02 M (according to the amount of MNP in mol) under nitrogen atmosphere. Two equivalents of APTES according to the amount of MNP were given to this suspension very carefully under vigorous stirring. The reaction was subsequently heated to 60 °C and incubated at 1000 rpm for 3 h. After cooling down to room temperature the particles were magnetically washed three times with 100 ml of EtOH and finally resuspended in 10 ml of H₂O_{dd}. The distribution of their diameter was 13.26 ± 4.32 nm as determined by dynamic light scattering (ZetaSizer Nano ZS, Malvern Instruments Ltd. Malvern, UK) with a number weighted distribution.

3.3. Cell preparation

MDA cells were transferred to a 24 Well plate 6 h before their loading with MNP. They were seeded with 80,000 cells per well, with 50,000 cells per ml and in quadruplets. The used MNP were added to the cells 100 pg Fe/cell for MNP, 80 pg Fe/cell for APTES-MNP and 20 pg Fe/cell for SO-Mag 5. After the incubation on a magnetic field for 24 h the cells were washed with PBS, resuspended in medium and transferred to Eppendorf tubes. Depending on their density each well was transferred to one tube, or two wells were combined into one.

3.4. Experimental set-up

For the observation of the cells, we designed a small set-up which can be placed under an inverted microscope. The layout of the set-up is shown in Fig. 1A. 47 small cuboidal rare-earth permanent magnets (height=50 mm, width=5 mm, NdFeB, N52; HKCM Engineering, Eckernförde, Germany) are arranged in two concentric Halbach cylinders (Inner array: 20 magnets on a circle with r =25.1 mm outer array: 27 magnets with r=33.1 mm). Thereby we achieved a quadrupole magnetic vector potential which would ideally lead to a perfectly uniform magnetic flux density and a constant magnetic gradient. However, due to the limited number of magnets, we only approximate such a field as shown in Fig. 1. Inside the set-up a standard cell culture dish (inner diameter=34 mm, polystyrene (PS)) is placed. The whole set-up is placed under an inverted microscope (Zeiss Axiovert 200, Carl Zeiss AG, Oberkochen, Germany) equipped with a digital CMOS camera (Hamamatsu C11440, Hamamatsu Photonics, Hamamatsu-shi, Shizuoka, Japan).

The vertical position of the inner bottom of the cell culture dish is fixed due to the construction of the magnetic set-up. Due to the added volume of the cell suspension another 0.8 mm can be added to the medium position of the object.

The magnetic gradient in the radial direction is therefore only approximately linear. Fig. 1B shows the magnetic flux density and Fig. 1C the magnetic gradient; both are shown in the plane perpendicular to the z-axis indicated in Fig. 1A. We achieve a magnetic gradient of approximately 23.7 T/m at the vertical center of the set-up. The observation window is at a radial position of 6 mm, where there is a very homogeneous magnetic field gradient.

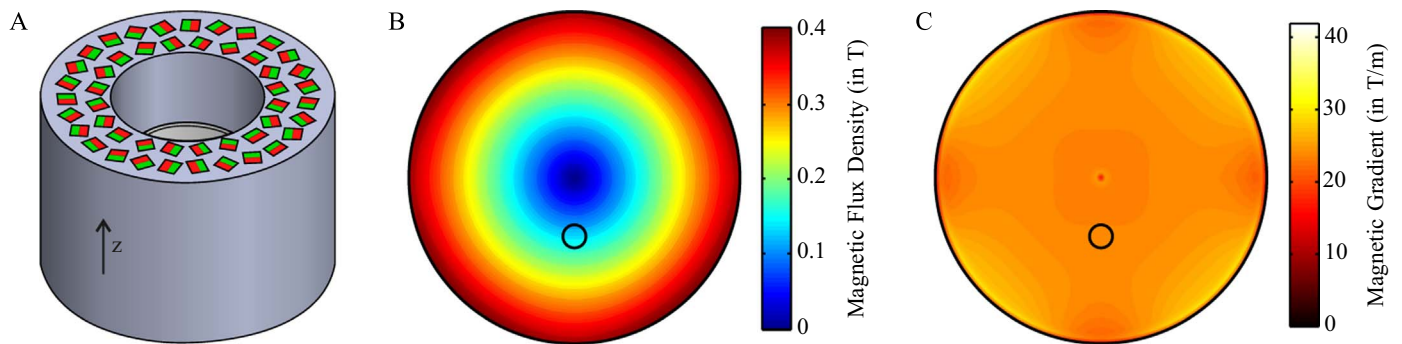


Fig. 1. Measurement set-up for magnetic moments of cells and microbubbles with mounting and cell culture dish (A): 47 permanent magnets are positioned in two circles around the cell culture dish where the colors indicate the poles of the magnets; magnetic flux density (B) and gradient of magnetic flux density in radial direction (C) inside the cell culture dish in the horizontal plane; small circle indicates observation window.

3.5. Magnetization measurement

The magnetic set-up was positioned under the inverted microscope and the obtained cell suspensions were transferred to a cell culture dish which was subsequently placed into the magnetic set-up. The movement of the objects was recorded at a 10 times magnification with a framerate of 5 fps. For each cell type, approximately 1500 images were recorded in multiple sets, with 130–140 images per set.

3.6. Evaluation

To evaluate the recorded images concerning object size and velocity, we use a custom tracking algorithm. The algorithm filters the image data, locates and identifies all objects matching certain conditions, and finally connects the individual objects over the image sequence. Thereby, the trajectories of the objects are reconstructed and we can evaluate the trajectory data. For more details on the algorithm, see [13].

The trajectories are evaluated concerning covered distance, velocity and size. From the positions throughout the image sequence, the recording frame rate and the scale, the velocity and the size of the objects can be deduced. Thereby, we can draw conclusions about the magnetic moment of the objects using Eqs. (2) and (5). Neglecting the acceleration of the particles, we can estimate the magnetic moment μ by the one-dimensional, radial equation

$$\mu_{\text{sat}} L(B(r)) \nabla_r B(r) = 3\pi\eta d_h v_r \quad (6)$$

where r denotes the radial position. To evaluate the magnetic moment and estimate errors, we use a χ^2 -fitting procedure [14] as described in [13].

4. Results

We performed several measurements with the above described set-up. In Table 1, we list the results for cell diameter, velocity, magnetic moment and volume magnetization. Values are given as mean value and standard deviation for normal distributions (in case of diameter)

Table 1
Results of measurements for MDA cells with different nanoparticles as mean value and standard deviation of the fitted distribution.

| Cell/ nanoparticle | Diameter (in μm) | Velocity (in $\mu\text{m/s}$) | Magnetic moment (in fA m^2) | Volume magnetization (in A/m) |
|-----------------------|---------------------------------|-----------------------------------|---|-------------------------------------|
| MDA MNP | 31.42 ± 3.29 | 1.85 ± 1.27 | 314.03 ± 419.70 | 15.08 ± 14.97 |
| MDA MNP- Aptes | 28.85 ± 4.11 | 3.30 ± 3.34 | 281.85 ± 298.18 | 23.60 ± 25.32 |
| MDA SO- Mag5 | 30.33 ± 3.16 | 2.00 ± 1.44 | 281.27 ± 355.65 | 19.17 ± 24.00 |

and arithmetic mean and standard deviation (for velocity, magnetic moment, volume magnetization). Fig. 2 shows the results exemplarily for MDA cells with MNP. Fig. 2A shows the reconstructed diameter, while B shows the measured velocity. The calculated magnetic moments as well as surface and volume magnetization are shown in Fig. 2C, D and E, respectively. The individual panels show the histogrammatic data for approximately 1400 trajectories, including the calculated errors as described above. The trajectories were extracted from approximately 1500 images. Additionally, we show a normal (in case of diameter) or lognormal distribution fitted to the data (for velocity, magnetic moment, volume magnetization).

We can see differences in the magnetic moment of the different cell and nanoparticle types. Fig. 2F shows the magnetic moments of the cells of Table 1 with respect to the used iron amount per cell. Though we used the least iron amount for SO-Mag5, the magnetic moment per cell is comparable to the moment of the cells incorporating MNP and MNP-APTES. Clearly, the intake of the magnetic nanoparticles by the cells is different for each cell and nanoparticle type.

5. Discussion and conclusion

Fig. 2 exemplarily shows the measurement and calculation results for MDA cells with MNP. The shown values were calculated individually for each reconstructed trajectory and subsequently fitted.

While all measured cell types share a normal distribution for the size distribution, the velocity, magnetic moment and magnetization follow a lognormal distribution. This most likely originates from the lognormal distribution of the nanoparticles. Furthermore, the distributions of diameter and magnetic moment cannot be transformed into the magnetization distribution by simple expressions. This indicated that the amount of incorporated nanoparticles is mainly independent of their size. Contrariwise, it could also be possible that the velocity and magnetic data follows a normal distribution, but is truncated and only appears as a lognormal distribution due to the close proximity of the peak value to zero. The movement of the lower half of the distribution might not have been recognized as movement. To investigate the exact correlation, a more detailed analysis with a higher time and space resolution would be necessary. Comparing the values in Table 1, one has to keep in mind that the arithmetic standard deviation of a lognormal distribution is not directly comparable to the one of a normal distribution and that the large values do not automatically correspond to larger errors.

Although there exist several similar methods to measure the magnetic moment or the magnetophoretic mobility of cells, most of them implicate that the cells are observed in flow. The most common method is to use a combination of one or multiple permanent magnets and a cell tracking velocimetry set-up. Zborowski and Chalmers et al. [5,6] used such a set-up in combination with paramagnetic particles. Those have a magnetic moment which is directly proportional to the

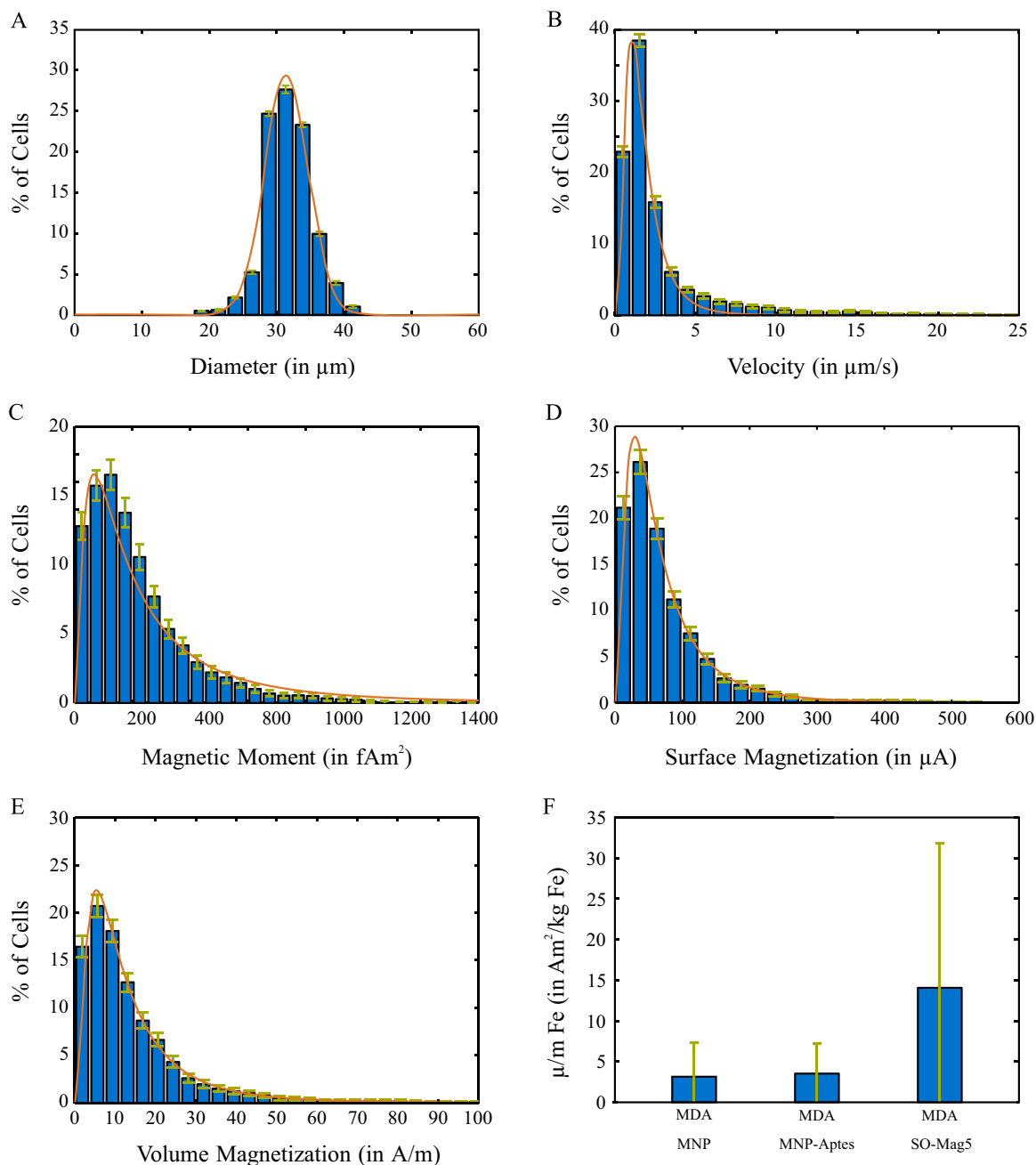


Fig. 2. Representative data from trajectory reconstruction of MDA cells with MN: diameter of cells (A), measured velocity (B) and calculated magnetic moment (C) as well as surface (D) and volume magnetization (E); the data evaluated from the microscopy images is displayed as blue bar plots with green error bars; the fitted distribution is shown as red lines. (For interpretation of the references to color in this figure legend, the reader is referred to the web version of this article.)

magnetic field. Their set-up is optimized to a constant gradient of the magnetic energy density which provides a constant force for paramagnetic nanoparticles. Häfeli et al. [4] as well as Wilhelm et al. [15] used a single permanent magnet to divert the particles perpendicular to their flow direction, thereby exerting a very inhomogeneous force. Under those circumstances, it is inadequate to neglect the acceleration due to the magnetic force.

While most of the cell tracking velocimetry set-ups are rather complicated, our only demand is the availability of an inverted microscope equipped with a digital video camera. In contrast to the described methods, we have a static environment for our objects, so we can safely assume that all observed long scale movement is due to the magnetic force. Additionally, we use containers where all optical planes are perpendicular to the light beam to avoid optical distortions. The design of a constant energy density gradient is not applicable in the

case of superparamagnetic nanoparticles. Even though the magnetic force can be approximated in a similar way, this is only valid for flux densities smaller than 50–100 mT. For magnetic flux densities larger than 200–300 mT, the magnetic moment can be approximated as constant. However, for the region between both approximations, the magnetic moment is not linearly dependent on the magnetic flux density and we need to include the known magnetic properties for the evaluation.

Nevertheless, we aimed for a constant force, by designing a set-up with a homogeneous magnetic gradient. However, the magnetic gradient is not completely homogeneous and the absolute value of the magnetic flux density is comparably small and varies strongly in the outer region of the cell culture dish. This is due to the limited height available under the microscope. As mentioned above, the Langevin behavior would have little to no influence on the magnetic moment for

higher magnetic flux densities, since this is equivalent to nanoparticles with a higher magnetic saturation. Thereby, such a set-up would be preferable. Nonetheless, we disregard the acceleration of the objects due to the non-homogeneous field gradient, similar to the measurements by Zborowski et al. and Häfeli et al.

Acknowledgements

A. Heidsieck and B. Gleich are supported by the “Deutsche Forschungsgesellschaft” (DFG) (grant no. GL 661/1-2) within the Research Unit 917 “Nanoparticle-based targeting of gene- and cell-based therapies”.

We thank J. Hinterrmair for technical support on cell culture. MNP- APTES were prepared by Jaroslaw Marcinişzyn. SO-Mag5 nanoparticles were kindly provided by O. Mykhaylyk (Institute of Experimental Oncology and Therapy Research, Klinikum rechts der Isar, Technische Universität München, Germany).

References

- [1] V. Kose, F. Melchert, *Quantenmasse in der Elektrischen Messtechnik*, VCH, Weinheim, 1991.
- [2] B. Morris, A. Wold, Faraday balance for measuring magnetic susceptibility, *Rev. Sci. Instrum.* 39 (1968) 1937–1941.
- [3] A. Saunderson, A permanent magnet Gouy balance, *Phys. Educ.* 3 (1968) 272.
- [4] U. Haefeli, M. Lobedann, J. Steingroewer, L. Moore, J. Riffle, Optical method for measurement of magnetophoretic mobility of individual magnetic microspheres in defined magnetic field, *J. Magn. Magn. Mater.* 293 (2005) 224–239.
- [5] M. Zborowski, J.J. Chalmers, *Magnetic Cell Separation*, Elsevier, 2007.
- [6] J.J. Chalmers, Y. Zhao, M. Nakamura, K. Melnik, L. Lasky, L. Moore, M. Zborowski, An instrument to determine the magnetophoretic mobility of labeled, biological cells and paramagnetic particle, *J. Magn. Magn. Mater.* 194 (1999) 231–241.
- [7] O. Mykhaylyk, O. Zelphati, J. Rosenecker, C. Plank, siRNA delivery by magnetofection, *Curr. Opin. Mol. Ther.* 10 (2008) 493.
- [8] O. Mykhaylyk, A. Steingotter, H. Perea, J. Aigner, R. Botnar, C. Plank, Nucleic acid delivery to magnetically-labeled cells in a 2D array and at the luminal surface of cell culture tube and their detection by MRI, *J. Biomed. Nanotechnol.* 5 (2009) 692–706.
- [9] A. Grief, Giles Richardson, Mathematical modeling of magnetically targeted drug delivery, *J. Magn. Magn. Mater.* 293 (2005) 455–463.
- [10] O. Mykhaylyk, T. Sobisch, I. Almstätter, Y. Sanchez-Antequera, S. Brandt, M. Anton, M. Döblinger, D. Eberbeck, M. Settles, R. Braren, D. Lerche, C. Plank, Silica-iron magnetic nanoparticles modified for gene delivery; A search for optimum and quantitative criteria, *Pharm. Res* 29 (2012) 1344–1365.
- [11] C. Rümmerapp, B. Gleich, H.G. Mannherz, A. Haase, Detection of molecules and cells using nuclear magnetic resonance with magnetic nanoparticle, *J. Magn. Magn. Mater.* 380 (2015) 271–275.
- [12] M. Ma, Y. Zhang, W. Yu, H.-y. Shen, H.-q. Zhang, N. Gu, Preparation and characterization of magnetite nanoparticles coated by amino silan, *Colloids Surf. A: Physicochem. Eng. Asp.* 212 (2003) 219–226.
- [13] A. Heidsieck, Simple Two-Dimensional Object Tracking based on a Graph Algorithm, *CoRR abs/1412.1216*, 2014.
- [14] W.H. Press, S.A. Teukolsky, W.T. Vetterling, B.P. Flannery, *Numerical Recipes: The Art of Scientific Computing*, Cambridge University Press, Cambridge, UK, 2007.
- [15] C. Wilhelm, F. Gazeau, J.-C. Bacri, Magnetophoresis and ferromagnetic resonance of magnetically labeled cells, *Eur. Biophys. J.* 31 (2002) 118–125.